

Original Article

# Histopathology of spontaneous lesions in FVB/N mice

Atsuko Murai<sup>1\*</sup>, Chisato Kaneko<sup>1</sup>, Hisakazu Sanada<sup>1</sup>, and Atsuhiko Kato<sup>1</sup>

<sup>1</sup> Safety and Bioscience Research Department, Translational Research Division, Chugai Pharmaceutical Co., Ltd. 216 Totsuka-cho, Totsuka-ku, Yokohama, Kanagawa 244-8602, Japan

**Abstract:** The FVB/N mouse strain is widely used in transgenic studies and as a model for autoimmune diseases. Although spontaneous lesions have been reported in aged FVB/N mice, information regarding younger FVB/N mice is lacking. This study aimed to investigate the spontaneous lesions in young FVB/N mice. Ten males and 10 females were necropsied at 10 and 26 weeks of age. All tissues were fixed in 10% neutral-buffered formalin, embedded in paraffin, and stained with hematoxylin and eosin. Histopathological examination revealed atrophy of the outer retina in all mice of both ages, with atrophy of the inner nuclear layer at 26 weeks. This ocular lesion is consistent with an autosomal recessive disorder in FVB/N mice. Decreased cellularity in the epiphyseal cartilage plate, reduced bone in the primary spongiosa of the femur, increased cellularity of lymphocytes in the thymus, dilatation of ducts in the mammary glands, and foveolar hyperplasia in the stomach were observed, all of which were indicative of age-related changes. These findings provide valuable background data for future studies using FVB/N mice. (DOI: 10.1293/tox.2024-0027; J Toxicol Pathol 2025; 38: 43–48)

**Key words:** FVB/N mice, background data, histopathology

## Introduction

FVB/N mice are widely used for transgenic studies because they produce many litters and their eggs have large prominent pronuclei<sup>1</sup>. This mouse strain is also used as a model for autoimmune diseases<sup>2–4</sup> and neurobiology<sup>5</sup>.

Spontaneous lesions have been reported in FVB/N mice aged 14 and 24 months. Alveolar-bronchiolar tumors were the most common neoplastic lesion, with a higher incidence than in other strains. Non-neoplastic lesions are characterized by chronic nephropathy, mononuclear cell infiltration in various tissues, and atrophic and degenerative changes in the ovaries, testes, and adrenal glands<sup>6</sup>. However, information on spontaneous lesions in young FVB/N mice is lacking. In transgenic studies, transgene-induced changes should be distinguished from background lesions in the original strain. The purpose of the present study was to identify spontaneous lesions in FVB/N mice aged 10 and 26 weeks old. The background data provided in this study can lead to a more insightful interpretation of the results of future transgenic studies using FVB/N mice.

## Materials and Methods

All animals were handled in accordance with the Guide for the Care and Use of Laboratory Animals at Chugai Pharmaceutical Co., Ltd., and all experimental protocols were approved by the Institutional Animal Care and Use Committee.

Forty, five-week-old FVB/NJcl mice (20 males and 20 females) were obtained from CLEA Japan, Inc. (Tokyo, Japan). Ten males and 10 females were necropsied at 10 and 26 weeks of age.

The mice were housed by group in mesh cages in a room maintained at 20 to 26°C, 30 to 70% humidity, 10 times/h air changes, with a 12-hour light dark cycle. The mice had free access to commercially available food (CRF-1, Oriental Yeast Co., Ltd., Tokyo, Japan) and tap water. The mice were euthanized by exsanguination under anesthesia and blood and tissues were collected. Urine was collected within one week of necropsy.

### *Hematology, blood chemistry, and urinalysis*

The following parameters were measured at each necropsy timepoint; red blood cell (RBC) count, hemoglobin (HGB), hematocrit (HCT), mean corpuscular volume (MCV), mean corpuscular hemoglobin (MCH), mean corpuscular hemoglobin concentration (MCHC), reticulocyte (RETIC), platelet (PLT) count, white blood cell (WBC) count and leukocyte differential of neutrophil (NEUT), lymphocyte (LYMPH), monocyte (MONO), eosinophil (EOS), and basophil (BASO) by blood (Automatic hematology ana-

Received: 29 March 2024, Accepted: 28 August 2024


Published online in J-STAGE: 11 September 2024

\*Corresponding author: A Murai

(e-mail: murai.atsuko79@chugai-pharm.co.jp)

©2025 The Japanese Society of Toxicologic Pathology

This is an open-access article distributed under the terms of the Creative Commons Attribution Non-Commercial No Derivatives

 (by-nc-nd) License. (CC-BY-NC-ND 4.0: <https://creativecommons.org/licenses/by-nc-nd/4.0/>).

lyzer XT-2000iV, Sysmex Corporation, Hyogo, Japan); aspartate aminotransferase (AST), alanine aminotransferase (ALT), alkaline phosphatase (ALP), glutamate dehydrogenase (GLDH), lactate dehydrogenase (LD), creatinine kinase (CK), total bilirubin (TBIL), total bile acid (TBA), urea nitrogen (UN), creatinine (CRE), glucose (GLUC), total cholesterol (TC), triglyceride (TG), total protein (TP), albumin (ALB), inorganic phosphorus (IP), calcium (Ca), sodium (Na), potassium (K), and chloride (Cl), and albumin/globulin (A/G) ratio by plasma (Automatic analyzer TBA-120FR, Canon Medical Systems Corporation, Tochigi, Japan); urine volume in 24-hour urine, sodium (Na), potassium (K), chloride (Cl), glucose (GLUC), and total protein (TP) by urine (Automatic analyzer TBA-120FR, Canon Medical Systems Corporation, Tochigi, Japan).

### Histopathological examination

The organs/tissues collected at necropsy were fixed in 10% neutral buffered formalin, which included the aorta, bone, and bone marrow of the femur, brain, eye, gallbladder, heart, small and large intestine, kidney, liver, lung, mammary gland, mesenteric lymph node, skeletal muscle, optic nerve, pancreas, sciatic nerve, skin, spleen, stomach, and thymus were processed, embedded in paraffin, sectioned, and stained with hematoxylin and eosin (HE) for histopathological examination.

## Results and Discussion

The hematology, blood chemistry, and urinalysis results are summarized in Tables 1–3. The WBC count at 26 weeks of age was lower than at 10 weeks of age, mainly due to a decrease in lymphocytes (Table 1). The lymphocytes count is known to decrease with aging<sup>7</sup>. The decrease in lymphocytes may affect the WBC count more significantly in this strain, as the percentage of lymphocytes in the WBC count is higher in FVB/N mice (Table 1) than in

normal mice<sup>7</sup>. Blood chemistry results showed that the ALT and AST levels were higher in 10-week-old males than in the other groups (Table 2), which was attributed to the very high levels in a single mouse (ALT, 780 U/L; AST, 264 U/L); however, there were no significant histopathological findings in the liver in this mouse.

Histopathological examination revealed lesions in the eye, femur, thymus, mammary gland, spleen, kidney, liver, and lung at 10 and 26 weeks of age, and in the stomach at 26 weeks of age (Table 4).

### Strain-specific findings

In the eyes, atrophy of the outer retina (Fig. 1) was observed in all mice of both ages, and atrophy of the inner nuclear layer (Fig. 2) was observed in all mice at 26 weeks of age. Retinal atrophy in FVB/N mice is reported as an autosomal recessive disorder exhibiting rapid degeneration of photoreceptors by postnatal day 35. In that study, the inner nuclear layer maintained its thickness at postnatal day 35, but a clear decrease was observed at 6 months of age<sup>7</sup>. Retinal atrophic lesions similar to those reported previously<sup>7</sup> were identified in the present study. Atrophy of the inner nuclear layer was evident at 26 weeks but not at 10 weeks. Thus, our investigation also supported this manner of progression of retinal atrophy in this mouse strain, over time.

### Age-related findings

In the femur, decreased cellularity in the epiphyseal cartilage plate (Fig. 3) was observed at 10 and 26 weeks of age, and the incidence increased with age. The hypertrophic zone was the most affected, and all zones were irregularly arranged, consistent with growth plate senescence<sup>8</sup>. A decreased bone area in the primary spongiosa (Fig. 4) was observed at 26 weeks of age. We were unable to find articles on the pathogenesis of the decreased bone area in the primary spongiosa of mice. In rats, decreased trabeculae has been reported as an age-related lesion<sup>9</sup>.

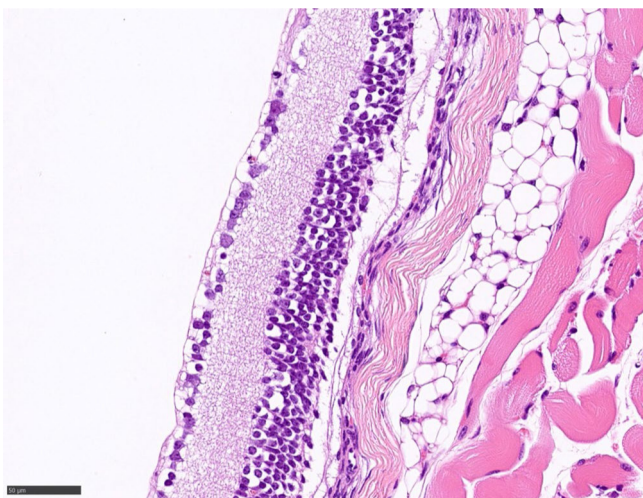


**Fig. 1.** Atrophy of outer retina in the eye. 10-week-old female FVB/N mouse. Bar=50  $\mu$ m.

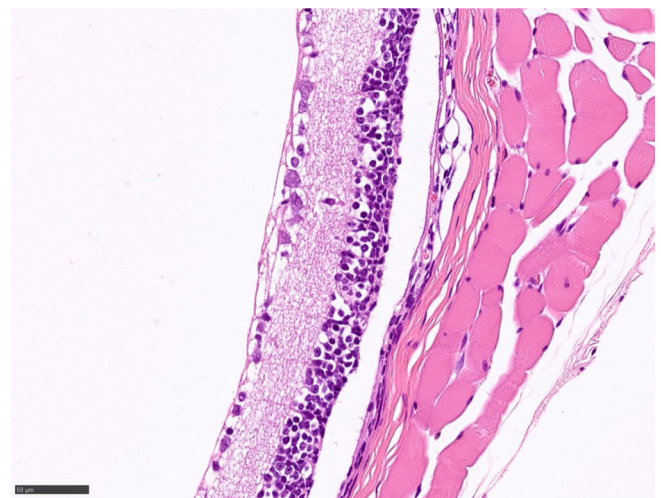


**Fig. 2.** Atrophy of inner nuclear layer in the eye. 26-week-old female FVB/N mouse. Bar=50  $\mu$ m.

**Table 1.** Hematological Data in FVB/N Mice

Weeks of age	Sex	Number of animals	RBC ( $10^6/\mu\text{L}$ )	HGB (g/dL)	HCT (%)	MCV (fL)	MCH (pg)	MCHC (g/dL)	RETIC (%)	PLT ( $10^3/\mu\text{L}$ )	WBC ( $10^3/\mu\text{L}$ )	NEUT (%)	LYMPH (%)	MONO (%)	EOS (%)	BASO (%)
10	Male	10	8.5 ± 0.3	12.8 ± 0.4	39.5 ± 1.5	46.3 ± 0.8	15.0 ± 0.1	32.4 ± 0.5	5.8 ± 0.7	1,486.3 ± 139.7	6.5 ± 1.4	7.4 ± 1.4	88.1 ± 1.5	3.6 ± 0.8	0.9 ± 0.6	0.0 ± 0.0
	Female	10	8.3 ± 0.3	12.7 ± 0.5	38.6 ± 1.5	46.5 ± 0.5	15.3 ± 0.1	32.9 ± 0.2	6.0 ± 1.2	1,453.1 ± 106.9	4.9 ± 0.9	6.9 ± 2.0	87.9 ± 2.4	4.2 ± 0.8	1.0 ± 0.3	0.0 ± 0.0
26	Male	10	8.4 ± 0.3	12.2 ± 0.6	38.1 ± 1.7	45.2 ± 0.9	14.5 ± 0.4	32.0 ± 0.7	5.3 ± 0.5	1,666.7 ± 60.0	3.0 ± 0.7	10.4 ± 3.7	85.4 ± 2.8	3.1 ± 2.0	1.2 ± 0.6	0.0 ± 0.1
	Female	10	8.1 ± 0.5	12.1 ± 0.7	37.4 ± 2.1	46.3 ± 0.8	15.0 ± 0.3	32.5 ± 0.3	4.4 ± 0.6	1,495.2 ± 101.6	2.5 ± 0.9	15.6 ± 3.1	78.4 ± 3.5	4.8 ± 1.5	1.2 ± 0.8	0.0 ± 0.0

Mean ± standard deviation. RBC: red blood cell; HGB: hemoglobin; HCT: hematocrit; MCV: mean corpuscular volume; MCH: mean corpuscular hemoglobin; MCHC: mean corpuscular hemoglobin concentration; RETIC: reticulocyte; PLT: platelet; WBC: white blood cell; NEUT: neutrophil; LYMPH: lymphocyte; MONO: monocyte; EOS: eosinophil; BASO: basophil.

**Table 2.** Blood Chemical Data in FVB/N Mice

Weeks of age	Sex	Number of animals	AST (U/L)	ALT (U/L)	ALP (U/L)	GLDH (U/L)	LD (U/L)	CK (U/L)	TBIL (mg/dL)	TBA ( $\mu\text{mol/L}$ )	UN (mg/dL)	CRE (mg/dL)	GLUC (mg/dL)	A/G ratio												
														TP (g/dL)	ALB (g/dL)	Ca (mmol/L)										
10	Male	10	68.0 ± 70.0	126.2 ± 231.3	105.1 ± 7.5	15.8 ± 6.7	431.1 ± 556.4	93.0 ± 64.6	0.1 ± 0.0	4.1 ± 5.1	25.0 ± 1.7	0.1 ± 0.0	285.7 ± 32.3	Female	10	56.3 ± 14.3	44.5 ± 19.4	102.4 ± 7.9	11.8 ± 3.5	263.2 ± 59.5	77.9 ± 38.0	0.1 ± 0.0	3.9 ± 2.7	24.5 ± 4.6	0.1 ± 0.0	261.6 ± 24.8
	Male	10	56.4 ± 14.1	50.7 ± 16.5	80.4 ± 8.3	13.4 ± 1.6	486.0 ± 162.2	471.6 ± 586.4	0.2 ± 0.0	4.0 ± 3.3	26.6 ± 1.9	0.1 ± 0.0	246.3 ± 42.1		Female	10	57.0 ± 12.9	32.8 ± 8.4	96.5 ± 13.7	12.6 ± 7.7	356.9 ± 135.4	284.6 ± 204.9	0.1 ± 0.0	5.2 ± 1.7	23.6 ± 3.2	0.1 ± 0.0
Weeks of age	Sex	Number of animals	TC (mg/dL)	TG (mg/dL)	TP (g/dL)	ALB (g/dL)	A/G ratio	IP (mg/dL)	Ca (mmol/L)	Na (mmol/L)	K (mmol/L)	Cl (mmol/L)	A/G ratio													
													TP (g/dL)	Na (mmol/L)	TP (mg/dL)											
10	Male	10	146.4 ± 9.5	163.2 ± 35.4	4.6 ± 0.1	2.8 ± 0.1	2.1 ± 0.8	6.5 ± 1.5	9.2 ± 0.4	143.7 ± 1.6	5.1 ± 0.7	110.2 ± 2.9	Female	10	135.6 ± 5.6	255.6 ± 104.1	4.7 ± 0.1	3.1 ± 0.1	2.0 ± 0.1	6.2 ± 0.7	9.0 ± 0.3	143.5 ± 1.2	4.6 ± 0.7	111.9 ± 1.0		
	Male	10	171.6 ± 12.3	250.2 ± 55.9	5.3 ± 0.3	3.4 ± 0.2	1.7 ± 0.2	6.2 ± 1.2	9.2 ± 0.4	144.0 ± 2.8	6.7 ± 0.5	108.3 ± 1.7		Female	10	129.9 ± 7.2	228.9 ± 83.0	5.4 ± 0.2	3.7 ± 0.1	2.2 ± 0.3	4.7 ± 1.0	8.7 ± 0.3	139.6 ± 2.5	5.3 ± 0.5	109.9 ± 1.7	

Mean ± standard deviation. AST: aspartate aminotransferase; ALT: alanine aminotransferase; ALP: alkaline phosphatase; GLDH: glutamate dehydrogenase; LD: lactate dehydrogenase; CK: creatine kinase; TBIL: total bilirubin; TBA: total bile acid; UN: urea nitrogen; CRE: creatinine; GLUC: glucose; TC: total cholesterol; TG: triglyceride; TP: total protein; ALB: albumin; IP: inorganic phosphorus; Ca: calcium; Na: sodium; K: potassium; Cl: chloride.

**Table 3.** Urinary Data in FVB/N Mice

Weeks of age	Sex	Number of animals	U.VOL (mL/24h)	Na (mmol/L)	K (mmol/L)	Cl (mmol/L)	GLUC (mg/dL)	TP (mg/dL)
10	Male	10	0.8 ± 0.4	214.2 ± 56.5	389.1 ± 70.2	315.3 ± 79.0	60.4 ± 10.6	1,220.6 ± 504.6
	Female	10	0.6 ± 0.3	195.8 ± 48.6	396.4 ± 78.3	321.3 ± 60.3	74.7 ± 15.6	225.8 ± 42.7
26	Male	10	0.7 ± 0.4	191.6 ± 26.4	431.6 ± 61.3	310.8 ± 50.7	77.0 ± 8.2	1,008.7 ± 489.8
	Female	10	0.8 ± 0.2	196.2 ± 38.5	385.8 ± 86.9	327.8 ± 70.3	65.3 ± 12.3	273.3 ± 60.0

Mean ± standard deviation. U.VOL: urine volume; Na: sodium; K: potassium; Cl: chloride; GLUC: glucose; TP: total protein.

**Table 4.** Number of Histopathological Findings in FVB/N Mice

Findings	10 weeks old		26 weeks old	
	Male (n=10)	Female (n=10)	Male (n=10)	Female (n=10)
Eye				
Atrophy of outer retina	10	10	10	10
Atrophy of inner nuclear layer	0	0	10	10
Femur				
Decreased cellularity in epiphyseal cartage plate	7	9	10	10
Decreased bone in primary spongiosa	0	0	10	6
Kidney				
Tubular hypertrophy	2	1	2	3
Mononuclear cell infiltration	2	1	3	1
Liver				
Focal necrosis	1	0	2	3
Lung				
Mononuclear cell infiltration in perivascular/vascular intima	1	1	4	0
Mammary gland				
Dilatation of duct	NE	4	NE	10
Spleen				
Brown pigment	10	10	10	10
Stomach				
Foveolar hyperplasia	0	0	7	7
Thymus				
Increased cellularity of lymphocyte in medulla	6	5	8	10

NE: not examined.

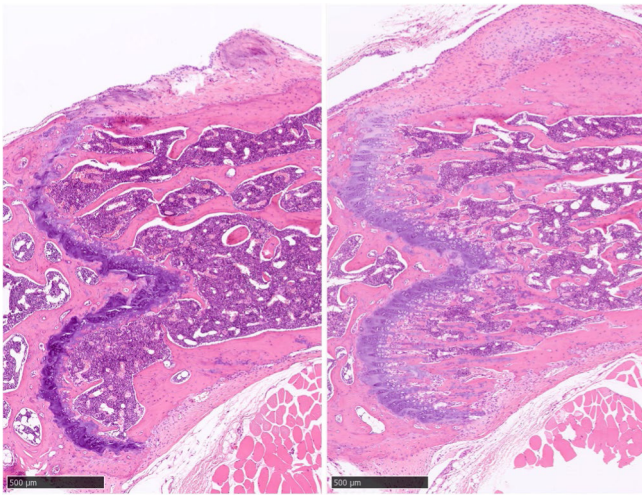


**Fig. 4.** Decreased bone area in the primary spongiosa in the femur of a 26-week-old male FVB/N mouse (left), compared with that of a 10-week-old male FVB/N mouse (right). Bar=500 µm.

In the thymus, increased cellularity of lymphocytes in the medulla (focal medullary B-cell hyperplasia) (Fig. 5) was observed in approximately 50% of mice at 10 weeks of age, and the incidence increased to almost 100% at 26 weeks of age. This lesion is associated with age-related involution<sup>10</sup>. Atypical hyperplasia is reported to be a pre-neoplastic lesion in chemically treated or p53 knockout mice

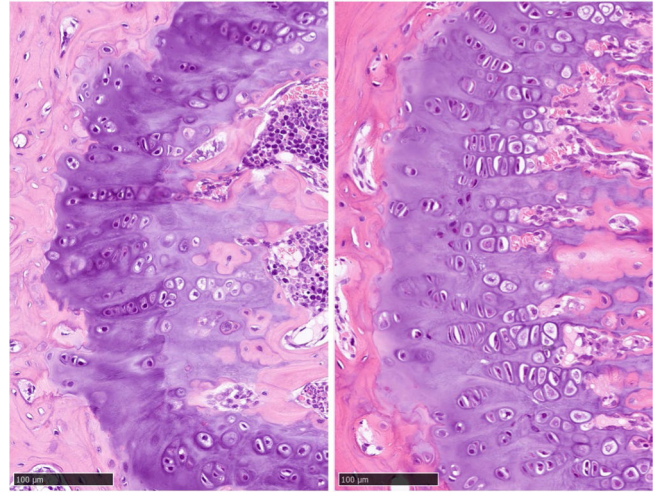


**Fig. 3.** Decreased cellularity in the epiphyseal cartilage plate in the femur of a 26-week-old male FVB/N mouse (left), compared with that of a 10-week-old male FVB/N mouse (right). Bar=100 µm.

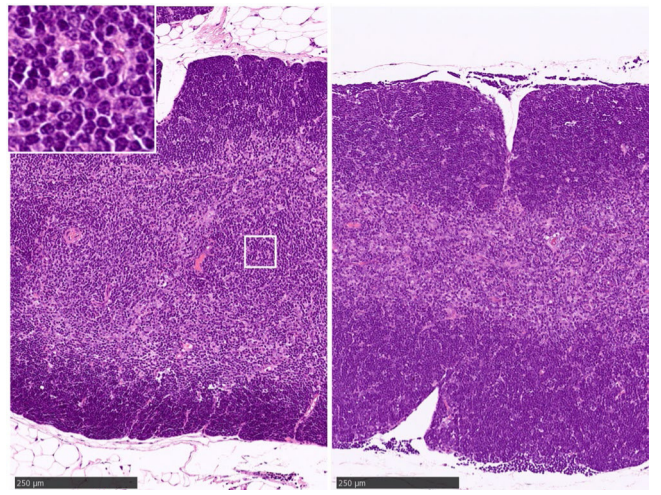


**Fig. 5.** Increased cellularity of lymphocytes in the medulla in the thymus of a 26-week-old female FVB/N mouse (left), compared with that of a 10-week-old female FVB/N mouse (right). Inset: higher magnification of the lymphocytes of a 26-week-old female FVB/N mouse. Bar=250 µm.

and is one of the differential diagnoses of increased cellularity. It consists of large and atypical lymphocytes and a variable cell population<sup>10</sup>. In the thymus, there was no cellular atypia in the increased lymphocytes. A previous study reported absence of lymphocytic tumors in FVB/N mice up to 14 months of age<sup>6</sup>. Therefore, increased lymphocyte cellularity in the medulla was deemed to be an age-related

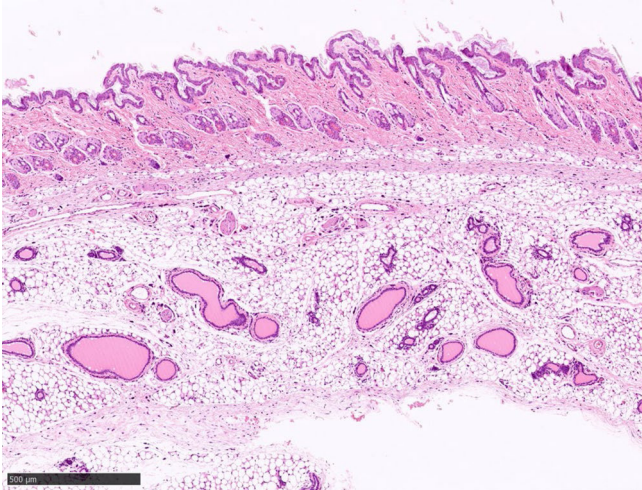


**Fig. 6.** Dilatation of ducts in the mammary gland. 26-week-old female FVB/N mouse. Bar=500  $\mu$ m.

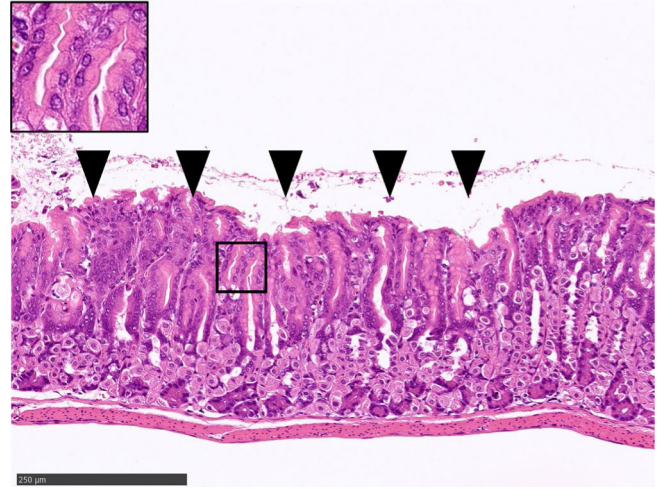


**Fig. 7.** Foveolar hyperplasia in the stomach (arrowheads). Insert: higher magnification of the surface mucous cells. 26-week-old male FVB/N mouse. Bar=250  $\mu$ m.

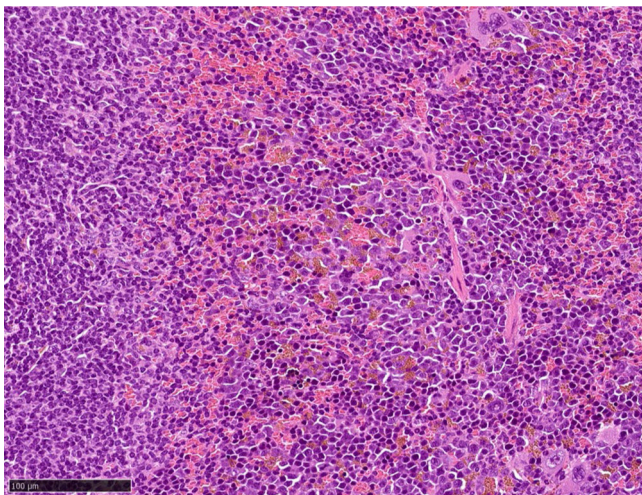


**Fig. 8.** Brown pigmentation in the red pulp in the spleen. 26-week-old female FVB/N mouse. Bar=100  $\mu$ m.

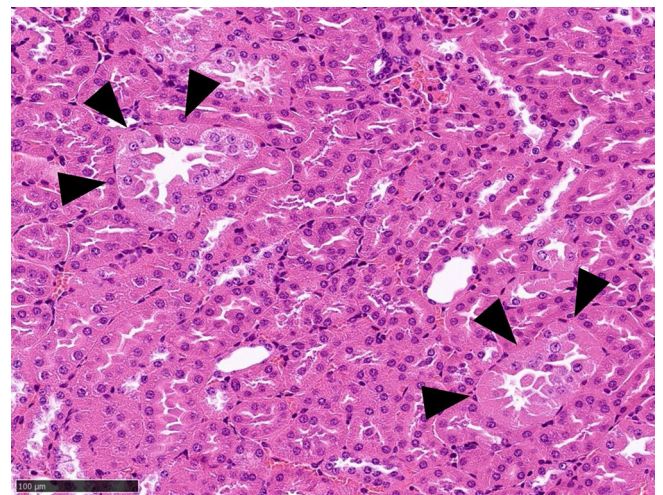


**Fig. 9.** Tubular hypertrophy in the kidney (arrowheads). 26-week-old male FVB/N mouse. Bar=100  $\mu$ m.

non-neoplastic change.

In the mammary glands of female mice, duct dilatation (Fig. 6) was observed in 40% of mice at 10 weeks of age and the incidence increased to 100% of mice at 26 weeks of age. Duct dilatation is an age-related condition associated with mammary gland hyperplasia and metaplasia<sup>11</sup>.

In the stomach, foveolar hyperplasia (Fig. 7) was observed in 70% of mice at 26 weeks of age, but not at 10 weeks of age. This lesion was composed of hyperplastic surface mucous cells containing abundant mucus. The proportion of gastric glands decreased due to surface mucous cell expansion, which resembled foveolar hyperplasia. In foveolar hyperplasia, surface mucous cells expand because progenitor cells in the isthmus proliferate, caused by an increased gastrin level<sup>12</sup>.

#### *Other findings*

The following findings were observed in the FVB/N mice at 10 and 26 weeks of age. In the spleen, all mice had brown pigmentation of the red pulp (Fig. 8). The pigmentation may be hemosiderin, lipofuscin, or melanin. In particular, hemosiderin accumulates in the spleen and bone marrow of aged mice during erythropoiesis<sup>10</sup>. The brown pigment in the red pulp observed in the present study was most likely to be hemosiderin. In the kidney, tubular hypertrophy (Fig. 9) and infiltration of mononuclear cells into the suburothelium were observed in some mice. Focal necrosis in the liver (Fig. 10) and mononuclear cell infiltration in the lung with distribution to the perivascular areas and vascular intima (Fig. 11) were observed in some mice.

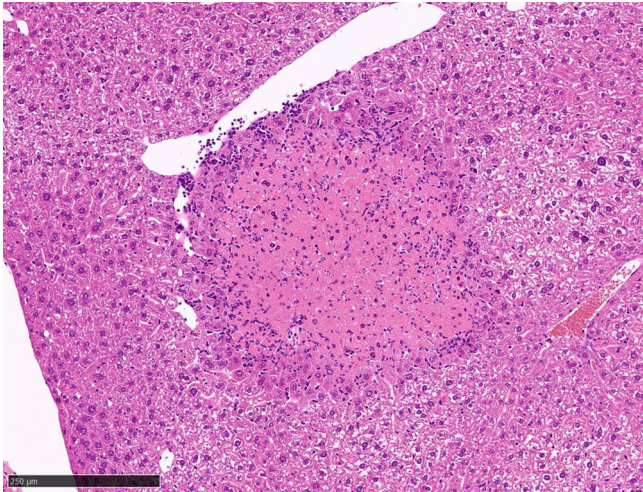


**Fig. 10.** Focal necrosis in the liver. 26-week-old female FVB/N mouse. Bar=250  $\mu$ m.

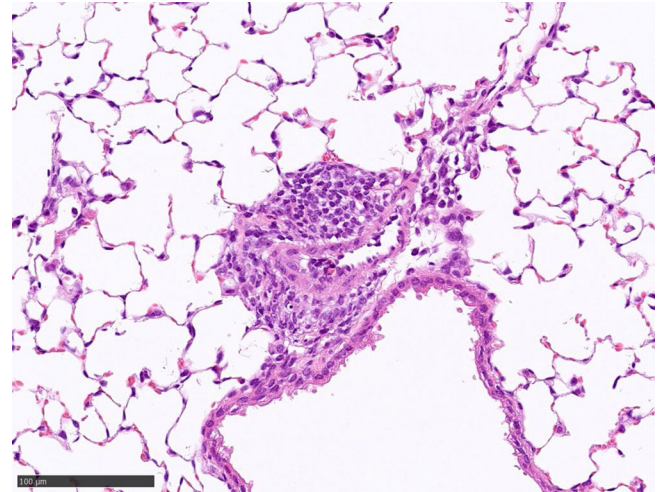


**Fig. 11.** Mononuclear cell infiltration in the perivascular and vascular intima in the lung. 10-week-old male FVB/N mouse. Bar=100  $\mu$ m.

### Conclusion

Histopathological examination of younger FVB/N mice revealed strain-specific findings in the eye; age-related findings in the femur, thymus, mammary gland, and stomach; and other findings in the spleen, kidney, liver, and lung. These findings provide valuable background data for future studies using FVB/N mice.

**Disclosure of Potential Conflicts of Interest:** In connection with this paper, the authors declare no potential conflicts of interest.

**Acknowledgments:** We thank Yuko Yamaguchi from the BoZo Research Center for the histopathological evaluation.

### References

1. Taketo M, Schroeder AC, Mobraaten LE, Gunning KB, Hanten G, Fox RR, Roderick TH, Stewart CL, Lilly F, Hansen CT, *et al* FVB/N: an inbred mouse strain preferable for transgenic analyses. *Proc Natl Acad Sci USA*. **88**: 2065–2069. 1991. [[Medline](#)] [[CrossRef](#)]
2. Holdener M, Hintermann E, Bayer M, Rhode A, Rodrigo E, Hintereder G, Johnson EF, Gonzalez FJ, Pfeilschifter J, Manns MP, Herrath M, and Christen U. Breaking tolerance to the natural human liver autoantigen cytochrome P450 2D6 by virus infection. *J Exp Med*. **205**: 1409–1422. 2008. [[Medline](#)] [[CrossRef](#)]
3. Murai A, Yamazaki M, Nishihara K, Kito A, Oyama S, Horiba N, and Kato A. Class II lupus nephritis with podocyte injury in imiquimod-induced lupus-prone mice. *Histol Histopathol*. **37**: 655–664. 2022. [[Medline](#)]
4. Yokogawa M, Takaishi M, Nakajima K, Kamijima R, Fujimoto C, Kataoka S, Terada Y, and Sano S. Epicutaneous application of toll-like receptor 7 agonists leads to systemic autoimmunity in wild-type mice: a new model of systemic Lupus erythematosus. *Arthritis Rheumatol*. **66**: 694–706. 2014. [[Medline](#)] [[CrossRef](#)]
5. Kasugai M, Akaike K, Imamura S, Matsukubo H, Tojo H, Nakamura M, Tanaka S, and Sano A. Differences in two mice strains on kainic acid-induced amygdalar seizures. *Biochem Biophys Res Commun*. **357**: 1078–1083. 2007. [[Medline](#)] [[CrossRef](#)]
6. Mahler JF, Stokes W, Mann PC, Takaoka M, and Maronpot RR. Spontaneous lesions in aging FVB/N mice. *Toxicol Pathol*. **24**: 710–716. 1996. [[Medline](#)] [[CrossRef](#)]
7. Yang J, Nan C, Ripps H, and Shen W. Destructive changes in the neuronal structure of the FVB/N mouse retina. *PLoS One*. **10**: e0129719. 2015. [[Medline](#)] [[CrossRef](#)]
8. Cole HA, Yuasa M, Hawley G, Cates JM, Nyman JS, and Schoenecker JG. Differential development of the distal and proximal femoral epiphysis and physis in mice. *Bone*. **52**: 337–346. 2013. [[Medline](#)] [[CrossRef](#)]
9. Fossey S, Vahle J, Long P, Schelling S, Ernst H, Boyce RW, Jolette J, Bolon B, Bendele A, Rinke M, Healy L, High W, Roth DR, Boyle M, and Leininger J. Nonproliferative and proliferative lesions of the rat and mouse skeletal tissues (bones, joints, and teeth). *J Toxicol Pathol*. **29**(Suppl): 49S–103S. 2016. [[Medline](#)] [[CrossRef](#)]
10. Willard-Mack CL, Elmore SA, Hall WC, Harleman J, Kuper CF, Losco P, Rehg JE, Rühl-Fehlert C, Ward JM, Weinstock D, Bradley A, Hosokawa S, Pearse G, Mahler BW, Herbert RA, and Keenan CM. Nonproliferative and proliferative lesions of the rat and mouse hemolymphoid system. *Toxicol Pathol*. **47**: 665–783. 2019. [[Medline](#)] [[CrossRef](#)]
11. Rudmann D, Cardiff R, Chouinard L, Goodman D, Küttler K, Marxfeld H, Molinolo A, Treumann S, Yoshizawa K. INHAND Mammary, Zymbal's, Preputial, and Clitoral Gland Organ Working Group. Proliferative and nonproliferative lesions of the rat and mouse mammary, Zymbal's, preputial, and clitoral glands. *Toxicol Pathol*. **40**(Suppl): 7S–39S. 2012. [[Medline](#)] [[CrossRef](#)]
12. Petersen CP, Mills JC, and Goldenring JR. Murine models of gastric corpus preneoplasia. *Cell Mol Gastroenterol Hepatol*. **3**: 11–26. 2016. [[Medline](#)] [[CrossRef](#)]